Supplementary information

Enhanced performance of piezoelectric composite nanogenerator based on gradient porous PZT ceramic structures for energy harvesting.

Huan Liu[a], Xiujuan Lin[a,*], Shuo Zhang[a], Yu Huan[b], Shifeng Huang[a,*], Xin Cheng[a]

[a] Shandong Provincial Key Laboratory Preparation and Measurement of Building Material, University of Jinan, Jinan 250022, PR China

[b] School of materials science and engineering, University of Jinan, Jinan 250022, PR China

* Corresponding authors. Email: mse_linxj@ujn.edu.cn (X. Lin)

The crystal structure of PZT particles, Chitosan and PZT/Chitosan was measured by X-ray diffraction (XRD, Bruker D8 Advanced, Germany) and FTIR spectrometer (FTIR, Thermo electron Nicolet 380, USA). XRD patterns and FTIR spectra were presented in Fig. S1. In the amorphous background of Chitosan, PZT particles and PZT/Chitosan showed the same diffraction peaks at 21.721°, 30.939°, 38.121°, 44.540°, 49.726°, 55.199° and 64.427°, which were derived from the (100), (101), (111), (200), (210), (211), and (022) planes of pure perovskite PZT (PDF 33-0784). In Fig S1(b), the broad absorption band at 3422 cm^{-1} existed in Chitosan and PZT/Chitosan, corresponding to the stretching mode of the free hydroxyl group (-OH). This came from the structure of Chitosan stabilized by intermolecular and intramolecular hydrogen bonds. In addition, the FTIR active modes coexisting between the two were provided in Table S1. These also indicated the presence of PZT and Chitosan. The composite did not change the crystal structure of the constituent phases, in other words, PZT and chitosan were better retained.

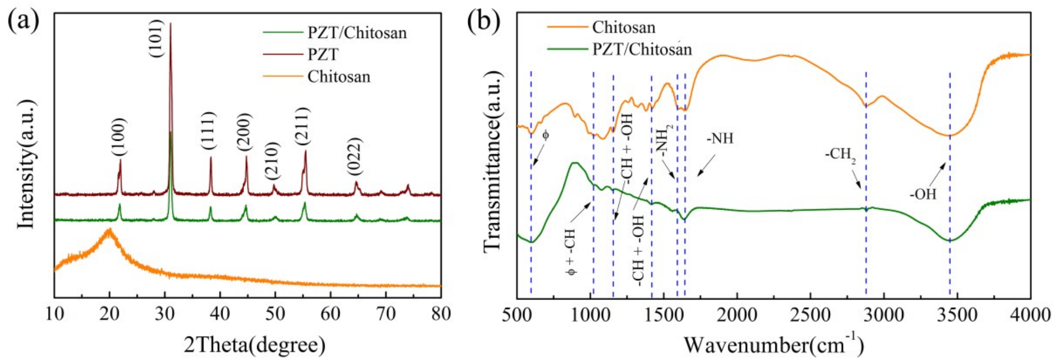

Fig S1 (a) XRD patterns of PZT particles, Chitosan and PZT/Chitosan and (b) FTIR spectra of Chitosan and PZT/Chitosan.

Table S1 FTIR active modes of Chitosan and its respective vibrations [54-57].

Number	Wavenumber(cm^{-1})	Observed(cm^{-1})	Assignment
1	3428	3428	ν(OH) Φ
2	2875	2875	$\nu(CH_2)$
3	1627	1627	δ(NH)chitin
4	1565	1583	$\delta(NH_2)$
5	1422	1423	δ(CH)+ δ(OH)
6	1156	1156	δ(CH)+ δ(OH)
7	1033	1022	ν(Φ)+ δ(CH)
8	595	594	δ(Φ)

A gradient porous structure was prepared using Chitosan of the same quality as in the PZT/ Chitosan backbone and encapsulated by using PDMS. When applying a force of 100 N to it, output voltage and current generated by Chitosan/PDMS composite were 16 V and 1.2 μA in turn, as shown in the Fig S2 below.

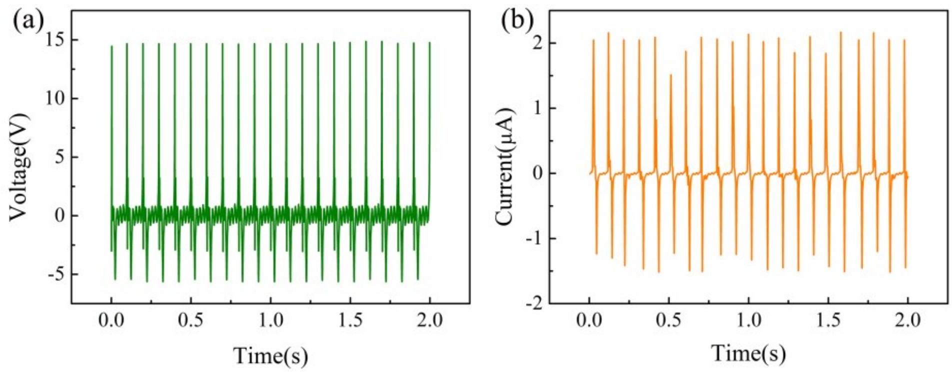

Fig S2 (a) Output voltage and (b) current of chitosan/PDMS composite.

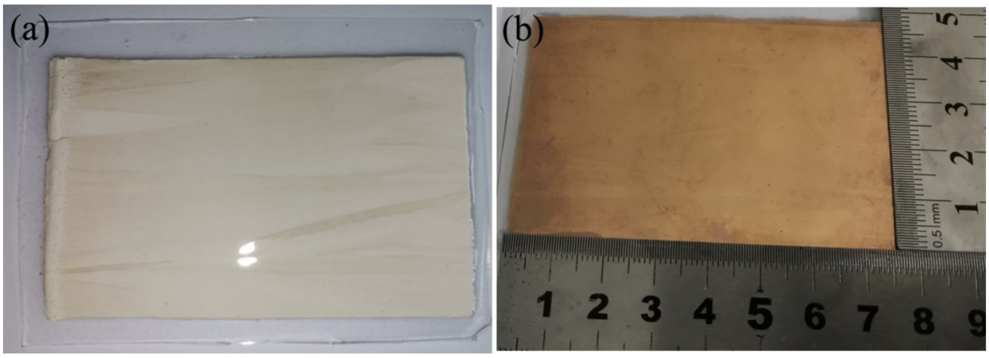

Fig S3 Physical pictures of (a) PZT/PDMS composite, (b) PZT/PDMS composite after coating Au.

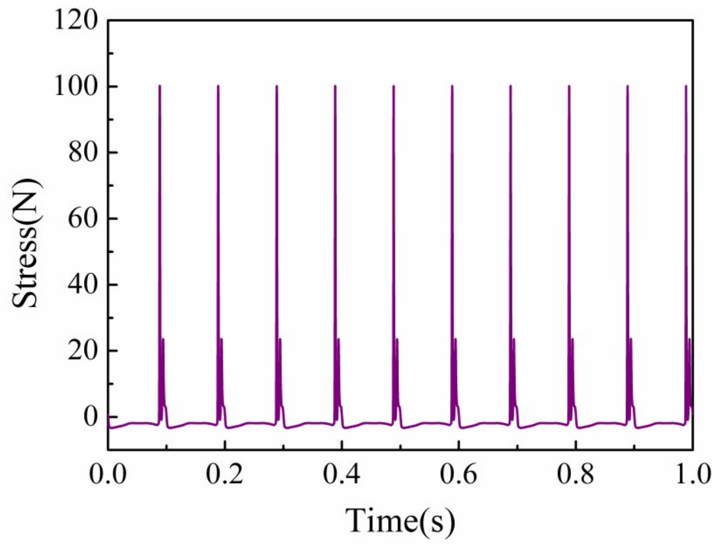

Fig S4 Stress applied on PZT/PDMS composite.

The gradient porous structure with size of 7.5 cm × 4.0 cm was prepared by freezing casting. Based on the mechanism of ice crystal growth and pores structure shape inside the ceramic, the device composed of regions with different structure morphologies, was divided into three parts in the direction of temperature gradient. At the same time, the central points of applied stress were called as C, B and A in sequence, as shown in Fig S5. In addition, a self-made excitation probe with a size of 4.0 cm × 2.5 cm (effective area of 10 cm^2) was used to impact the regions where C, B, and A were located.

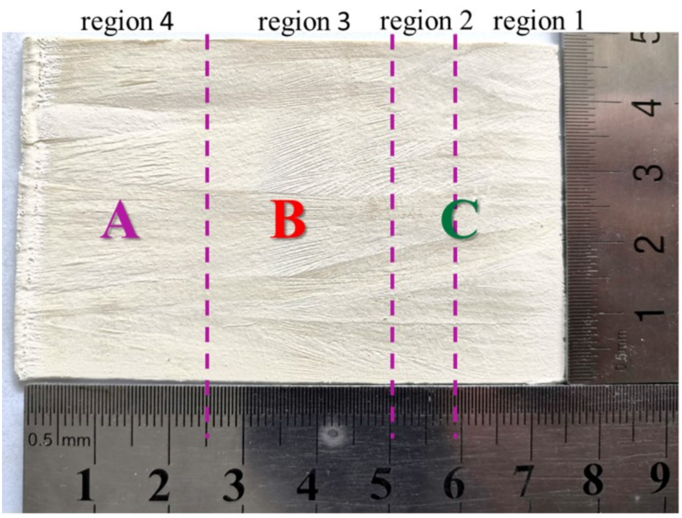

Fig S5 Physical picture of gradient porous structure after freeze-dried.

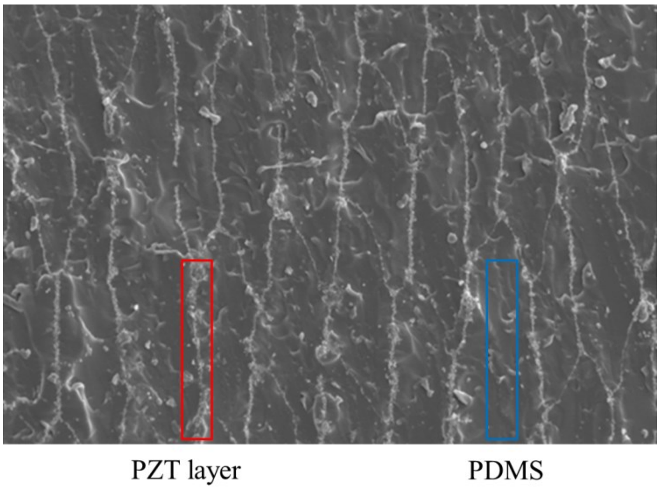

Fig S6 Cross image of gradient porous PZT/PDMS composite.

In order to more clearly explore the gradient characteristics of the porous PZT backone, SEM images were analyzed by using Image-Pro Plus and Nano Measure. As shown in Fig S7. The porosity and pore size of different regions was calculated in backbone of 1.9 vol% PZT/PDMS composite. Along the freezing direction of the temperature field, the analyzed porosity was approximately 44%, 61% and 78%，respectively. And average size of pores was 17.49 μm, 35.35 μm and 50.56 μm in turn. Clearly, both porosity and pore size also exhibited increasing trend, indicating the gradient of the porous structure. Therefore, for gradient structure in this work, it referred to a gradient size and porosity within the composite.

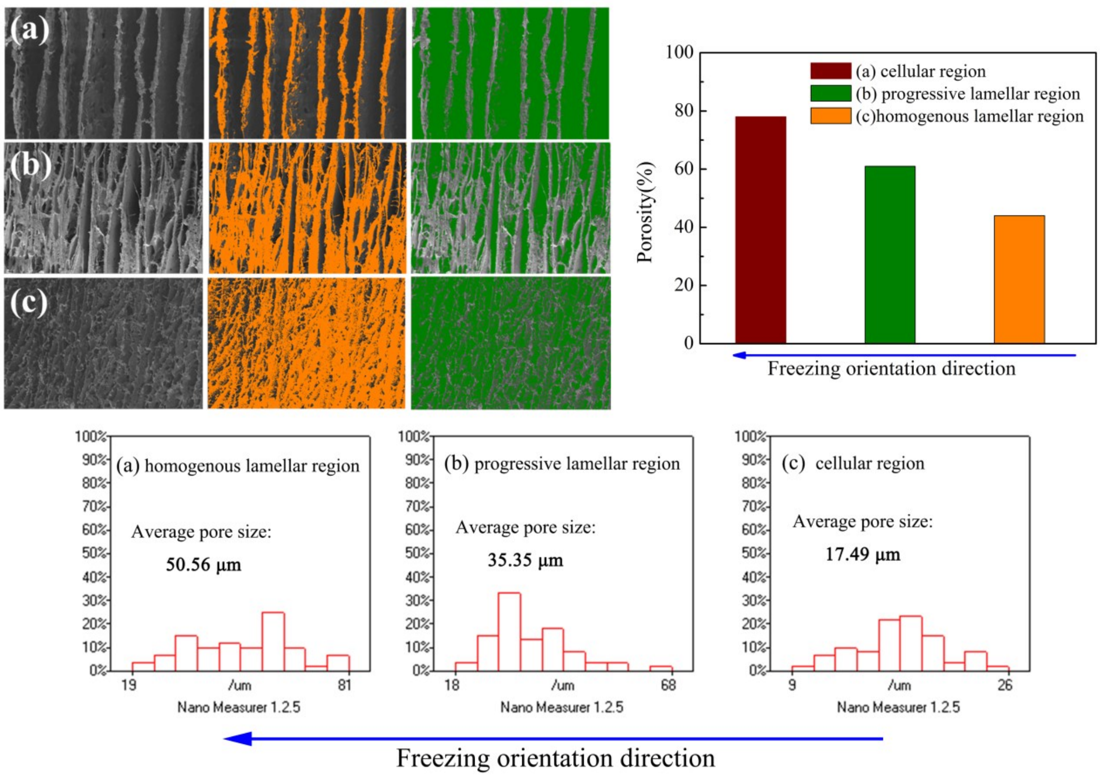

Fig S7 Porosity and pore size expression of different region formed along the freezing orientation direction in backbone of 1.9 vol% PZT/PDMS composite.

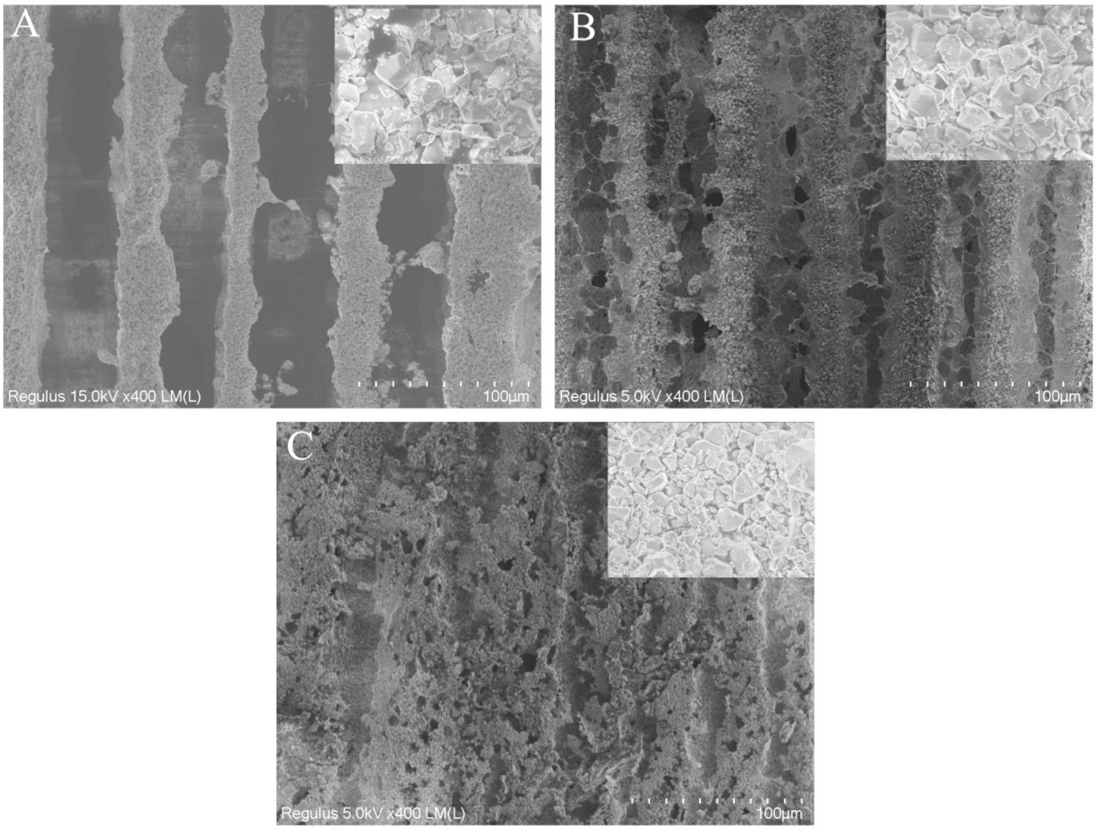

Fig S8 Microstructure images in backbone of 6.5 vol% PZT/PDMS composite at A, B and C (Inset: SEM images of particle distribution).

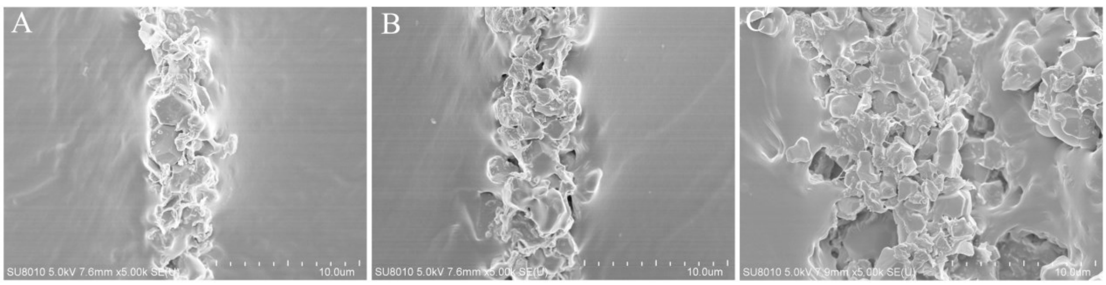

Fig S9 SEM image of interface of 6.5 vol% PZT/PDMS composite at A, B and C.

Table S2 Performance comparison of different composites based PENGs.

composites	Filler's content	thickness	Applied stress	Poled electrical field	Frequency（Hz）	Power density(μW/cm2)	Ref.
Oriented BN NT/P(VDF-TrFE)	0.3 wt%	---	40N	10kV/mm at 90	2	11.3	46
PZT NP/PVDF	30 wt%	---	Finger tapping	---	4	36	47
Porous interconnected BT BP/PDMS	---	300 μm	32 N	150kV/mm at 100℃	3	2.95	27
Aligned P(VDF-TrFE) NF/PMMA	---	3 mm	2 kPa	---	1.5	8.75	48
KNN-BZN-AS-Fe NP/PDMS	40 wt%	---	25 N	10 kV/mm at 50℃	2	3.63	49
3D interconnected Sm-PMN-Pt NP/PDMS	---	500 μm	35 N	80kV/cm	0.2	11.5	15
KNN NP/Ag/CNT/PDMS	10wt%	1 mm	100 N	10 kV/mm at 100℃	1	141.25	11
3D interconnected BFO NP/PDMS	30 wt%	---	35 N	6 kV/mm at 70℃	3	3.11	17
BT NP/PDMS	10 wt%	2 mm	Bending	20 kV/cm at 100℃	---	9.741	50
BT NP/P(VDF-TrFE)	40 wt%	---	Bending	10 kV/mm at R.T.	---	13.5	51
3D-skeletal BCTZ/PDMS	20 wt%	100 μm	0.2 MPa	---	0.2	2	29
BTNW/CNT/PDMS	40 wt%	3 mm	247 N	50 kV/cm at 140℃	11	107.5	52
Gradient porous PZT NP/PDMS	5.2 vol%	2 mm	100 N(0.1MPa)	8 kV/mm at 100℃	10	110	This work
Gradient porous PZT NP/PDMS	5.2 vol%	2 mm	80 N(0.08MPa)	8 kV/mm at 100℃	10	72.6	This work
Gradient porous PZT NP/PDMS	5.2 vol%	2 mm	50 N(0.05MPa)	8 kV/mm at 100℃	10	33.6	This work
Gradient porous PZT NP/PDMS	5.2 vol%	2 mm	30 N(0.03Mpa)	8 kV/mm at 100℃	10	21.7	This work
Aligned pt-PVDF	---	---	0.3Mpa	---	5	22	53
Porous interconnected CNF/PDMS	---	480 μm	0.05MPa	---	10	210	28